Path- and Area-Integrated Rainfall Measurement by Microwave Attenuation in the 1–3 cm Band

DAVID ATLAS[1]

National Center for Atmospheric Research[2], Boulder, Colo. 80303

CARLTON W. ULBRICH

Department of Physics and Astronomy, Clemson University, Clemson, S. C. 29631

(Manuscript received 14 September 1976, in revised form 27 September 1977)

ABSTRACT

The reasons for the linear relationship between microwave attenuation A and rainfall rate R near 1 cm wavelength are explained. This linearity also implies independence of the A-R relationship from the drop size distribution (DSD), thus making attenuation measurements near this wavelength attractive for path-averaged rainfall. Regression equations of the form $A = KR^{\alpha}$ are calculated for four radar wavelengths from 0.86 to 3.2 cm from drop size spectra. As predicted, α increases from about 1.04 to 1.16 and average errors of estimate of R from the regression equations increase from about 9 to 21% from 0.86 to 3.2 cm, respectively. The larger errors at 3.2 cm reflect the increased dependence on the form of DSD. Even at 3.2 cm, the errors are typically less than half those incurred from the use of reflectivity factor Z and *a priori* Z-R relations.

Various methods of measuring path- and area-averaged R are studied. Radar methods using standard targets fail over 30 km paths at wavelengths of 0.86 and 1.25 cm at $\bar{R}$ greater than about 9 and 20 mm h^{-1}, respectively, because of excessive attenuation but are operative to larger mean rates at 1.78 and 3.2 cm. One-way methods between transmitter and receiver are the most suitable in terms of maximum measureable $\bar{R}$. A wavelength between 1.5 and 2 cm provides a reasonable compromise between maximum measurable $\bar{R}$ and minimum errors. Proper measurements require the use of both vertical and horizontal polarization. Prior experiments are reviewed and explanations offered for both the large scatter in the results of some experiments and the occasional excess attenuation over theoretical prediction.

1. Introduction

It has long been known that microwave attenuation A by rainfall near wavelengths of 1 cm is nearly linearly related to rainfall rate (Ryde, 1947; Wexler and Atlas, 1963). This was the basis for several experiments to measure path-integrated rainfall at 0.86 cm using two or more known targets along a path [Collis and Lidga, 1961; Godard, 1965; Harrold, 1967; also see discussion in Atlas (1964)]. Some of these experiments achieved reasonable success. Recently Atlas and Ulbrich (1974) and Ulbrich and Atlas (1977a, b), hereafter referred to as I and II and III, respectively, have argued that since any parameter which depends on the drop size distribution (DSD) involves at least two distribution parameters such as the number concentration and a representative drop size, two independent measurements are necessary to reduce the errors of estimate of rainfall rate R from those which are obtainable with a single measurement such as radar reflectivity factor Z and an *a priori* choice of a Z-R relation. The basis for such improved measurements of R was established in I and II through the development of a rain parameter diagram, and the utility of the method was demonstrated in III.

In this paper, we investigate the theoretical reasons for the linear A-R relationship near 1 cm and also show that the A-R function is essentially independent of the DSD at such wavelengths. We demonstrate these points empirically using actual DSD's and investigate the errors in R as a function of wavelength. We also describe several practical configurations for measuring path- and area-averaged rainfall and their limitations. Finally we review some prior experiments and attempt to account for discrepancies from theory.

2. Theory

The attenuation of any beam of radiation by a medium of scatterers is given by

$$A = 0.4343 \int_0^{\infty} N(D) Q_t(D) dD, \qquad (1)$$

[1] Present affiliation: NASA Goddard Space Flight Center, Greenbelt, Md. 20771.

[2] The National Center for Atmospheric Research is sponsored by the National Science Foundation.

Unauthenticated | Downloaded 04/21/25 09:47 PM UTC

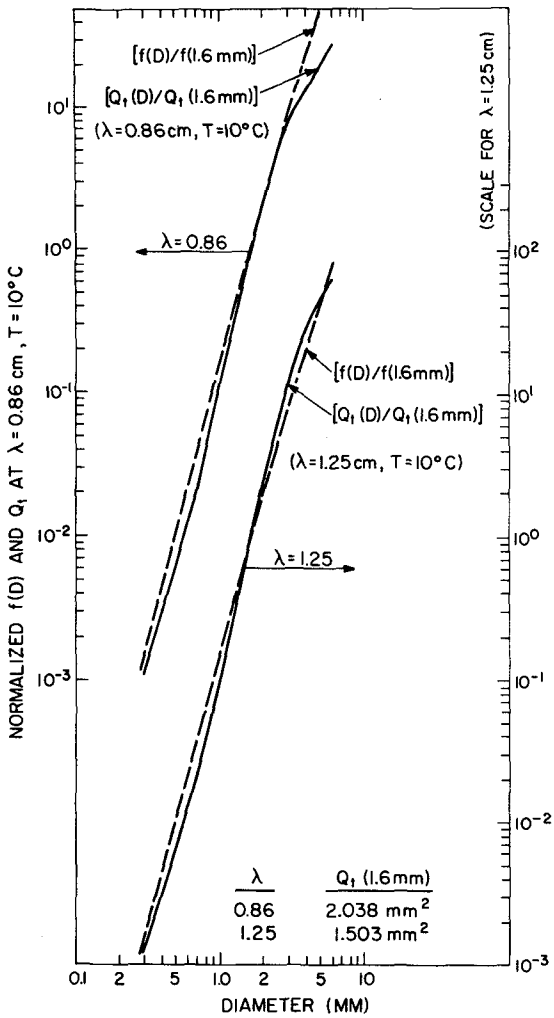

FIG. 1. The weighting functions $f(D)$ and $Q_t(D)$ at 0.86 and 1.25 cm for R and A, respectively, normalized at $D=1.6$ mm.

where A is the attenuation (db km^{-1}), $N(D)$ the DSD (m^{-3} cm^{-1}) and $Q_t(D)$ the total extinction cross section (cm^2) of the drops of diameter D (cm). In I, we have shown that for most practical purposes the complex behavior of $Q_t(D)$ can be expressed by a power law fit of the form

$$Q_t(D)=CD^n \tag{2}$$

over the range of drop sizes which contribute significantly to A. Indeed we have shown in I that any power law regression equation between A and R or between A and M (liquid water content) such as have appeared in the literature (Wexler and Atlas, 1963; Eccles and Mueller, 1971) must imply a $Q_t(D)$ power law such as Eq. (2). Using Eq. (2) in Eq. (1) yields

$$A=0.4343C\int_0^\infty N(D)D^n dD. \tag{3}$$

In I, we have computed values of C and n for a wide range of wavelengths and temperatures.

The rainfall rate R (mm h^{-1}) is given by

$$R=6\times10^{-3}\pi\int_0^\infty N(D)v(D)D^3dD, \tag{4a}$$

where $v(D)$ is the raindrop fallspeed (cm s^{-1}), or

$$R=6\times10^{-3}\pi\int_0^\infty N(D)f(D)dD, \tag{4b}$$

where $f(D)=v(D)\ D^3$ is the weight of the contribution of drops of diameter D to R. The fallspeed law at standard temperature and pressure was given by Atlas *et al.* (1973) as

$$v(D)=965-1030\exp(-6D)\ [\text{cm s}^{-1}]. \tag{5}$$

This is an excellent fit to the data of Gunn and Kinzer (1949). Thus

$$f(D)=D^3[965-1030\exp(-6D)]. \tag{6}$$

This function, normalized to its value at $D=0.16$ cm, is plotted in Fig. 1 on a log-log scale; it fits the power law

$$f(D)=1767D^{3.67}\ [\text{cm}^4\ \text{s}^{-1}],\ 0.05<D<0.5\ \text{cm}. \tag{7}$$

Dividing by D^3, we also find from Eqs. (5) and (6) that the fallspeed may also be expressed as a power law of the form

$$v(D)=1767D^{0.67}\ [\text{cm s}^{-1}],\ 0.05<D<0.5\ \text{cm} \tag{8}$$

which is close to that proposed by Sekhon and Srivastava (1971) but significantly different from that of Spilhaus (1948). Using Eq. (7) in Eq. (4b), we find

$$R=6\times10^{-3}\pi(1767)\int_0^\infty N(D)D^{3.67}dD. \tag{9}$$

Comparing Eqs. (9) and (3), we see that the integrands would be identical if the exponent n in (2) and (3) were equal to 3.67. Referring to Fig. 1 and Table 1 of I we find $n=3.67$ at a radar wavelength $\lambda=0.88$ cm; at 0.86 cm, $n=3.65$. This table also shows that at this wavelength C and n are essentially independent of temperature over the range 0–18°C

TABLE 1. Comparison of exponents α in $A=KR^\alpha$.

λ (cm)	This work ($T=10$°C)	Atlas and Ulbrich (1974) ($T=10$°C)	Wexler and Atlas (1963) ($T=0$°C)
0.86	1.04	1.01	1.0
1.25	1.10	1.08	1.07
1.778	1.13	1.14	—
1.87	—	—	1.10
3.22	1.16	1.23	1.15

Unauthenticated | Downloaded 04/21/25 09:47 PM UTC

and are altered only negligibly as the temperature rises to 40°C. Thus, at wavelengths of 0.85 to 0.9 cm the integrals in (3) and (9) will be virtually identical and A will be a linear function of R, *essentially independent of the form of* $N(D)$, *the DSD and of the temperature.*

To demonstrate how well the slopes of the $Q_t(D)$ and $f(D)$ laws match at radar wavelengths near 0.9 cm we also plot $Q_t(D)$ (normalized at $D=1.6$ mm) on Fig. 1 for a wavelength of 0.86 cm and a temperature of 10°C using the Mie attenuation cross sections for $Q_t(D)$. The two curves match very well indeed up to drop sizes of about $D=3.2$ mm. At larger sizes the slope of $Q_t(D)$ decreases and the curve begins to fall significantly below that of $f(D)$. Fig. 1 also shows a similar comparison of $f(D)$ to $Q_t(D)$ at $\lambda=1.25$ cm. Here, too, the match is good, but $Q_t(D)$ falls somewhat above $f(D)$ in the range $2<D<4$ mm. Thus, when we use the exact Mie attenuation cross sections for $Q_t(D)$ we again find that A will be linearly dependent on R at wavelengths between 0.86 and 1.25 cm, with very slight dependence on the DSD.

In Fig. 2 we show loci of the percentage cumulative contributions to both R and A for a Marshall and Palmer (1948) (hereafter referred to as MP) distribution at $\lambda=0.86$ and $\lambda=1.25$ cm. The dashed curves correspond to R, solid curves to A. They were computed using the fallspeed law [Eq. (6)] in Eq. (4b) for R, the Mie attenuation cross sections for $Q_t(D)$ in Eq. (1), and the MP exponential DSD for $N(D)$. The loci match reasonably well over a wide range of R. If we compare the loci of $0.95R$ and $0.95A$, we see that significant differences begin to occur at

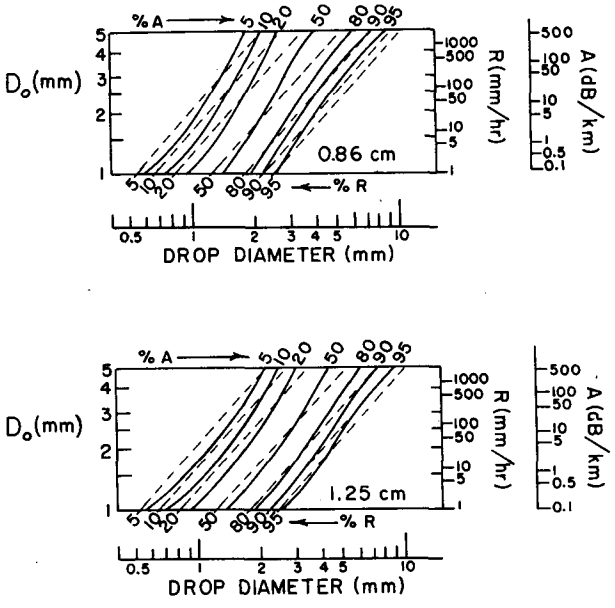

FIG. 2. Isopleths of cumulative percent contribution to R and A by drops smaller than abscissa (R, dashed; A, solid) for $\lambda=0.86$ (top) and 1.25 cm (bottom).

$R\gtrsim 50$ mm h^{-1}, but these differences are probably unrealistic because the remaining fractional contributions are due to drops larger than about 3.5–4 mm whose number concentrations are generally overestimated in the MP DSD. In any event, the power law fit to $Q_t(D)$ at 0.86 cm tends to overestimate the actual extinction coefficients for $D>3$ mm so that the linear A-R relationship derived therefrom will slightly overestimate the actual rainfall rate at large rainfall rates. This is true regardless what form the DSD takes.

We may find the A-R relation for an MP DSD interpolating from the values in Table 1 of I at 0.86 cm and 0–18°C. This results in

$$A\ [\text{dB km}^{-1}]=0.237\ R^{1.01}. \tag{10}$$

The exponent is insignificantly different from 1.0. Using $C=16.7$ (from Fig. 1 in I) in Eq. (3) and equating the integrals in (3) and (9) we get $A=0.217\,R$ which is sufficiently close to Eq. (10) considering the approximations. The coefficient in (10) compares to a value of 0.27 computed by Wexler and Atlas (1963) for an MP DSD at 0°C. However, examination of their A-R curve shows that a value of about 0.25 is a better average over the entire range $0.1<R<100$ mm h^{-1}. Using the DSD data of Kelkar (1961), Godard (1965) calculated both R and A at 0.86 cm and found $A=0.29\,R$. However, his actual attenuation experiments give $A=0.23\,R$ for $R\leqslant 9.5$ mm h^{-1}. The latter is in excellent accord with Eq. (10).

3. Empirical evidence

In order to confirm the linear A-R law predicted above at $\lambda\approx 0.9$ cm, we have numerically computed exact values of A and R for 204 DSD's. Each of these DSD's is the average of seven consecutive 1 min DSD's on each of three days in 1974 which shall be referred to here as days 174, 195 and 220. The observations were taken in Locarno, Switzerland, by Joss, who graciously provided the data to us. A description of the disdrometer with which these data were taken is given by Joss and Waldvogel (1967). Values of A were computed at wavelengths of 0.86, 1.25, 1.778 and 3.22 cm and $T=10$°C using Eq. (1) and the Mie attenuation cross sections for $Q_t(D)$. The resulting scattergrams and lines of best fit found by performing a log-log regression to an equation of the form $A=KR^{\alpha}$ are shown in Fig. 3. The regression equations and the average percent deviation of R regardless of sign are shown in the upper inset table of Fig. 3. In the lower inset table we give the linear A-R relations obtained by a log-log fit to $A=KR$, and the associated average percent deviation of R from these linear A-R laws.

We see that at $\lambda=0.86$ cm, the best-fit regression equation is $0.219\,R^{1.04}$ with an average deviation of only 8.8% in R. This is in excellent agreement with

Unauthenticated | Downloaded 04/21/25 09:47 PM UTC

the expected relationship given by Eq. (10). As predicted in I, the exponents on R increase with radar wavelength. A comparison of the exponents found in this work with those predicted in I and by Wexler and Atlas (1963) for an MP DSD is shown in Table 1. The small differences between the α's found here and those of other workers are due, of course, to the difference between the actual average DSD and the MP DSD. The difference in α at 3.22 cm between I and Wexler and Atlas (1963) is due in part to the temperature difference. It is interesting to note that Ryde (1947, Fig. 7) calculated $A=0.19\,R$ at $\lambda=1.0$ cm and $T=18$°C for a Laws and Parsons DSD.

Note also (Fig. 3, top inset table) that the percentage errors in R from the regression equations increase with wavelength and with the exponent on R. This is a manifestation of the increasing dependence on the DSD as wavelength is increased and the $Q_t(D)$ function deviates more and more from $f(D)$ [Eqs. (6) and (7)].

When we force linear fits to the data of Fig. 3, the lower inset table also shows that the percent error in R from the linear relation increases by only 2% to a value of 10.8% at 0.86 cm. Moreover, most of this increase is due to the smallest R's. However, use of the linear fits at the other wavelengths increases the average errors by a factor of about 2. At 0.86 cm we may therefore use the linear relation

$$A=0.228\,R \tag{11}$$

without incurring appreciably greater errors than with the power law equation.

We have investigated the degree to which the errors in R can be further reduced through the use of a rain parameter diagram for $\lambda=0.86$ cm like that shown in I and II. This involves a dual-measurement method similar to that tested in III wherein the DSD is assumed to be an MP distribution, i.e., of the form

$$N(D)=N_0 e^{-\Lambda D}, \tag{12}$$

where $N_0(\mathrm{m^{-3}\ cm^{-1}})$ and $\Lambda(\mathrm{cm^{-1}})$ are parameters of the distribution. When this form for $N(D)$ is used in Eq. (1) for A and in

$$Z=10^6\int_0^\infty D^6 N(D)\,dD \tag{13}$$

for the radar reflectivity factor $Z(\mathrm{mm^6\ m^{-3}})$ at a radar wavelength for which the Rayleigh approximation is valid, the resultant expressions form a system of two equations for the unknowns N_0 and Λ in terms of A and Z. Consequently, unique solutions can be found for N_0 and Λ and for any other precipitation parameters defined in terms of these parameters, e.g., $R=R(N_0,\Lambda)=R(Z,A)$. These solutions are unique because they do not require the introduction of empirical relations (e.g., Z-R) or the equivalent

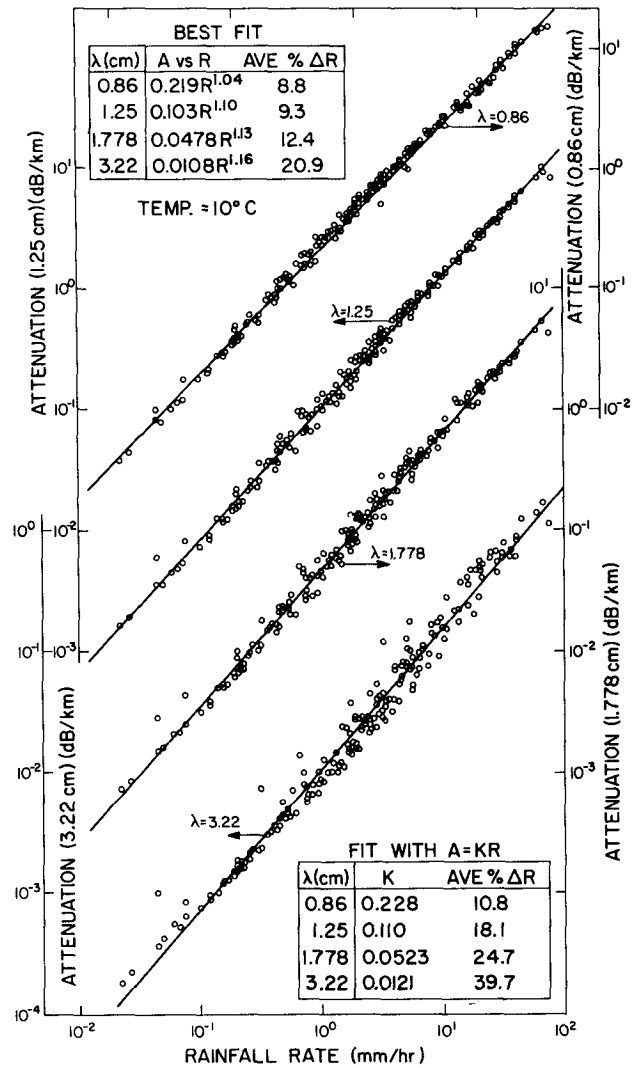

FIG. 3. Scattergrams and regression lines of A vs R at indicated wavelengths. Inset tables give regression equations and average errors in R (see text).

alternative of invoking assumptions about the dependence of N_0 or Λ on rainfall rate. It has been shown in III that such a dual-measurement method can considerably reduce the errors in R relative to that which results from the use of empirical relations. The application of this method using Z and A to find R for the drop size spectra described above produces an average error of 5.0%, or 3.8% less than that obtained from A alone with the line of best fit, and 5.8% less than that obtained with the linear fit of Eq. (11). The three methods are compared at the bottom of Table 2. Thus, unless one is interested in extreme precision, a dual-measurement method using A and Z is hardly necessary at $\lambda=0.86$ cm, at least for path-averaged rainfall.

For purposes of comparing these results with those found by estimating R from Z alone, Table 2 lists

Unauthenticated | Downloaded 04/21/25 09:47 PM UTC

TABLE 2. Z-R and A-R relations and average percent rainfall errors (all data for 1974). Attenuation at $\lambda=0.86$ cm, T=10°C.

Day	Z-R	A-R	Average error in R (%): Using actual Z-R law	Average error in R (%): Using JW Z-R law
174	$321\ R^{1.44}$		27.2	26.7
195	$376\ R^{1.39}$		44.6	44.8
220	$456\ R^{1.47}$		23.7	41.5
All 3	$377\ R^{1.42}$		34.1	35.5
All 3		$0.221\ R^{1.04}$	8.8	
All 3		$0.228\ R$	10.8	
All 3	Dual-measurement method $R=R(A,Z)$		5.0	

the Z-R regression equations for the three individual days of measurement, the combined Z-R relation for all three days, the rainfall errors incurred by using these equations, and those incurred by using the *a priori* relation $Z=300\ R^{1.5}$ of Joss and Waldvogel (1970) (hereafter referred to as JW). Also shown are the errors incurred from the use of the A-R relationships and the dual-measurement method described above. We see that the errors resulting from the use of the Z-R laws are some three to four times as large as those obtained from the 0.86 cm A-R relation even if we have some way of determining what the appropriate daily Z-R relation is. However, since there is no good method of determining the Z-R relationship in advance, we would have to assume one like that of JW. We see that this approach produces no appreciable change in the errors on days 174 and 195 because the JW empirical Z-R law is appropriate on these days. However, on day 220, the average error is almost doubled because of the systematic difference between the JW Z-R law and that for this day. Needless to say, the errors resulting from the use of the 0.86 cm A-R relations will not vary appreciably from day to day because of the slight dependence on the DSD.

4. Some practical methods

In this section we describe several techniques for measuring path-averaged rainfall rates by attenuation which take advantage of the results found in the previous sections. As a practical example we shall use the specifications of the 0.86 cm AN/TPQ-11 radar system to determine the maximum measurable average rainfall rate.

a. Two-way radar methods

In these methods the two-way path attenuation is measured with a radar and fixed target of known cross section. The maximum permissable path loss L is then determined from the radar equation as

$$L\ [\mathrm{dB}]=-10\ \log[(P_{\min}(4\pi)^3X^4)/(P_tG_0^2\lambda\sigma N^{\frac{1}{2}})], \quad (14)$$

where $P_{\min}$ is the minimum detectable power of the radar, P_t the peak transmitted power, λ the wavelength, G_0 the axial gain of the radar antenna, and X the distance to the target of cross section σ. In addition, N is the number of signals integrated; the square root dependence assumes incoherent integration. The maximum average rainfall rate along the path is then found from

$$\bar{R}_{\max}=L/2KX, \quad (15)$$

where K is the coefficient of the linear A-R relation (cf. inset, Fig. 3). We have determined $\bar{R}_{\max}$ for four different two-way radar methods using the characteristics[3] of the AN/TPQ-11 and assuming a 10 s integration time ($N=10^4$). The radar and target are taken to be 50 ft above the ground so that $X=30$ km which is just within the radar horizon. The four methods considered are as follows:

1) METHOD A

The target is a shorted paraboloid identical to the radar antenna with cross section $\sigma=G_0A_g$, where A_g is the antenna area. For wavelengths other than 0.86 cm we scale the antenna and target diameters proportional to wavelength.

2) METHOD B

Same as method A except that the target is kept constant in diameter and equal to that at 0.86 cm. This is desirable for economic reasons when a multiplicity of targets is to be viewed by the radar.

3) METHOD C

Same as method B except that the target is a frequency shift reflector (FSR) (Chisholm, 1963) returning signals to the radar different from that of the rain and ground clutter. This method provides a stable known target independent of meteorological conditions at the target.

4) METHOD D

Same as method B but the targets are 10 m² flat plates. Their advantage is ease and economy of production.

For all of these methods we find $\bar{R}_{\max}\approx 10$, 20, 40 and 200 mm h^{-1} for radar wavelengths of 0.86, 1.25,

[3] For the AN/TPQ-11, $P_t=1.2\times10^5$ W, $P_{\min}=10^{-13}$ W, $\lambda=0.86$ cm, $G_0=4.0\times10^5$ (56 dB), antenna diameter $D=2.13$ m, geometric aperture $A_g=3.58$ m², effective aperture $A_e=2.37$ m², pulse width $\lambda=0.5$ μs, pulse repetition frequency PRF=10^3 s^{-1} and receiver bandwidth=2 MHz.

Unauthenticated | Downloaded 04/21/25 09:47 PM UTC

1.778 and 3.22 cm, respectively. If X is halved to 15 km, these become $\bar{R}_{max} \approx 20$, 40, 100 and 400 mm h^{-1} but this decrease in X greatly reduces the areal coverage. Note that the largest measurable $\bar{R}_{max}$'s occur at 3.22 cm but this wavelength suffers from the largest errors in R and the results are temperature dependent (see I, Table 1). However, considering the fact that the path-averaged DSD will greatly reduce the scatter in Fig. 3 and that corrections can be made for the temperature dependence, this wavelength is surely useful for measurement of intense rains. A wavelength of 1.788 cm appears to be suitable for measurement of all but the most intense rainfall rates.

A practical configuration might employ a radar at the center of a circle of 30 km radius with 36 standard targets distributed at 10° intervals around the perimeter of the circle. The targets could be any of those described or combinations thereof.

b. One-way methods

A one-way path can be used for measurement of intense rainfall rates or when only a few paths are required. In this case L is given by

$$L\ [\text{dB}] = XK\bar{R}_{max} = -10 \log[P_{min} 4\pi X^2/(P_t G_0 A_{er} N^{\frac{1}{2}})], \quad (16)$$

where A_{er} is the effective aperture of the receiving antenna. Again using the characteristics of the AN/TPQ-11 and an equivalent receiving antenna, and scaling the results to wavelengths other than 0.86 cm by increasing the diameters of the antennas proportional to wavelength, we find $\bar{R}_{max} \approx 25$, 50, 100 and 500 m h^{-1} for wavelengths of 0.86, 1.25, 1.778 and 3.22 cm, respectively, and $X = 30$ km. These results are, of course, larger than those found for the two-way methods with $X = 30$ km, but the method requires the use of a single transmitter and a multiplicity of receivers. The transmitter would be considerably cheaper than a radar (e.g., it could be a CW transmitter) but the cost would increase with the number of receivers. Another approach would be to transmit from the ground to a receiver on board an aircraft flying a constant range circle on the far side of a storm. The attenuation profile would then be an image of the azimuthal variation of average rainfall rate.

We have also devised a one-way zig-zag path involving one transmitter, two receivers and eight flat plate reflectors to cover a square area 30 km on a side as shown in Fig. 4. A simple extension of Eq. (16) for a one-way path permits us to determine $\bar{R}_{max}$ for this configuration. The results are $\bar{R}_{max} \approx 1$, 3, 6 and 26 mm h^{-1} for wavelengths of 0.86, 1.25, 1.778 and 3.22 cm, respectively. Although these appear to be small, these averages are now over a 150.8 km path. The corresponding equivalent rainfall rates which could be measured over any one of the paths between reflectors are 7, 14, 30 and 130 mm h^{-1}.

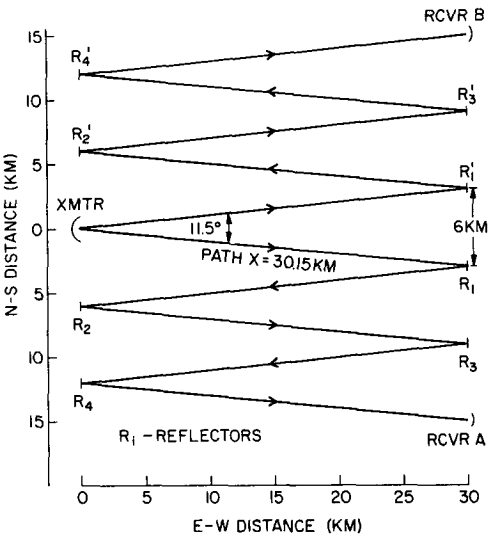

FIG. 4. Zig-zag method for area-integrated rainfall.

5. Rainfall statistics for 30 km paths

In order to estimate the utility of any of the aforementioned methods, one should have some idea of the number of hours per year during which 30 km path-averaged rainfalls will exceed the $\bar{R}_{max}$'s found in the previous section. Drufuca (1974) has provided such attenuation-duration data for Montreal for one-way paths up to 15 mi (24 km) at $\lambda = 2.68$ cm. We have converted his 2.68 cm attenuation curves (his Fig. 2) to path average rainfall using the relation $L = 0.021\ \bar{R}X$ [dB], where the coefficient is interpolated from the inset table in Fig. 3, and have extrapolated his curves smoothly to a path length of 30 km. The resulting curve, which is an approximation at best, is shown in Fig. 5. Lenhard (1974) provides similar statistics over longer paths in Illinois; however, for a 30 km path his Fig. 2 extends only to 40 mm h^{-1}. We also show this portion of the Illinois curve in Fig. 5. It is surprisingly close to that for Montreal, crossing the latter at about 30 mm h^{-1}.

The approximate maximum path-averaged rain rates measurable by each of the methods in Section 5 are shown in Fig. 5 for the four wavelengths considered in this work. For the zig-zag method we use the equivalent 30 km rain rates, assuming for this purpose that only one of the paths will be filled. (A more rigorous approach would require finding the joint probability that all five paths were filled by rain of intensity one-fifth as great.) It is seen that at 3.2 cm, all methods function successfully; they fail less than 10^{-3} hours per year. However, this is achieved at a loss in sensitivity in measuring light rains. If we require that the system fail less than only 1 hour per year, then we may use the 1.778 cm two-way radar method or any of the one-way techniques except at 0.86 cm. Since the 1.778 cm one-way method fails less than 0.006 hour per year, such a system will

Unauthenticated | Downloaded 04/21/25 09:47 PM UTC

undoubtedly function successfully in more intense rain climates than that in Montreal. This wavelength also provides greater sensitivity to lighter rains than 3.22 cm.

6. Other concerns

a. Correction for nonspherical drops

We have investigated the effects of the increasing ellipticity of raindrops as they become larger by using the results of Oguchi and Hosoya (1974). They have computed the attenuation for vertical polarization (A_V) and for horizontal polarization (A_H) at $\lambda=0.86$ cm and $T=20°C$ for a variety of raindrop canting angles. Their results for horizontally oriented oblate spheroids are shown in Fig. 6 together with the empirical linear A-R law [Eq. (11)] we deduced earlier for spherical drops. For $50 \lesssim R \lesssim 110$ mm h^{-1} the linear A-R law almost precisely bisects the A_H and A_V curves of Oguchi and Hosoya. For these conditions the differential attenuation varies with R as $A_H - A_V = 0.039\,R$ as shown in Fig. 6 which gives a one-way differential attenuation of about 40 dB along a 10 km path at $R=100$ mm h^{-1}. Clearly, then, in order to make the most accurate measurements of R we should make measurements of both A_H and A_V using a circularly polarized transmitting antenna, or alternately on both polarizations. In principle, the linearity of $A_H - A_V$ with rainfall rate would permit the use of differential attenuation as a measure of rainfall rate. However, the difference $A_H - A_V$ decreases as the raindrop canting angle becomes smaller. Since the canting angle is unlikely to be constant over an extended path one may conclude that accurate measurements of path-averaged R can be achieved by making measurements on both polarizations and using the average of A_H and A_V with the linear A-R law deduced in this work.

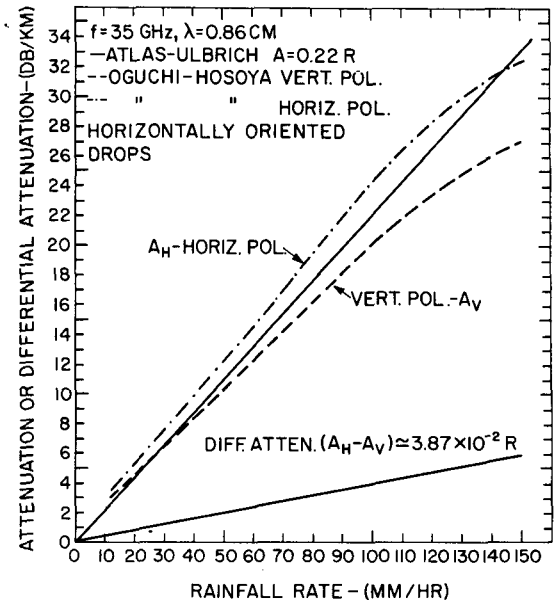

FIG. 6. Attenuation at 0.86 cm for both polarization corresponding to oblate raindrops (curves) and spheres (straight line). Bottom line, differential attenuation (see text).

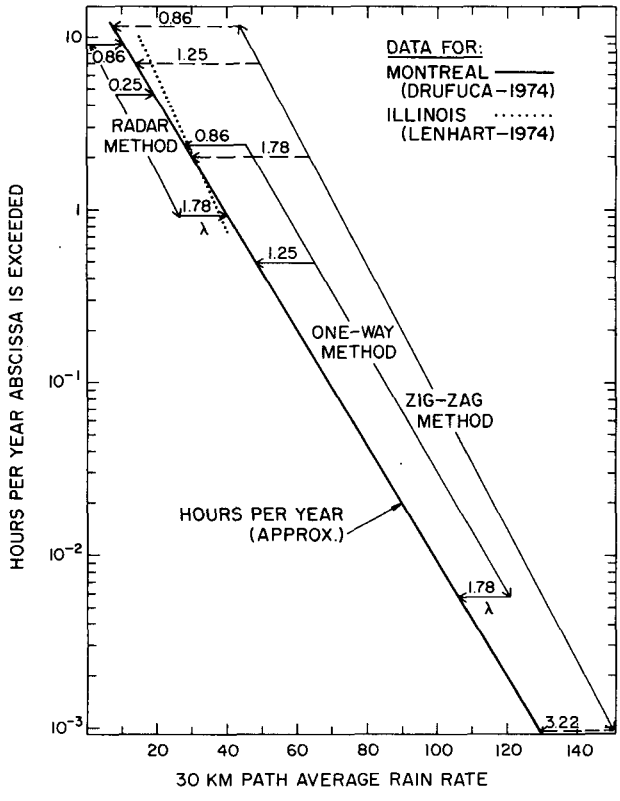

FIG. 5. Hours per year that 30 km path $\bar{R}$ is exceeded in Montreal and Illinois. Horizontal arrows indicate maximum $\bar{R}$ measurable at each wavelength by methods shown.

b. Errors due to nonlinear A-R dependence

The linear dependence of A on R at 0.9 cm wavelength makes it possible to use the total path loss as a direct measure of $\bar{R}$ independent of the form of the distribution of R along the path. However, when the A-R law is nonlinear, small errors are incurred. Using the relationship

$$A = K\bar{R}^{\alpha}_{\text{est}} = (K/2X)\int_{-X}^{+X} [R(x)]^{\alpha} dx, \qquad (17)$$

where $\bar{R}_{\text{est}}$ is the estimated average rainfall rate, we have computed the percentage error from the true average for rainfall profiles of parabolic and isosceles triangular shape. The results are given in Table 3. We see that small deviations in α from 1 produce only small overestimates of the true $\bar{R}$; also the errors are not too sensitive to the form of the rainfall profile.

Unauthenticated | Downloaded 04/21/25 09:47 PM UTC

c. *Multiple scattering*

At high frequencies and large rainfall rates, Crane (1971) believes that multiple scattering begins to affect the received signals on incoherent transmission paths (i.e., those in which the receiver is not phase-locked to the transmitter). Coherent transmission systems are not so affected because the multiply scattered signals have random phases with respect to the attenuated direct signals. Crane also notes that the effect is to enhance the received signal above that which would be observed otherwise. This occurs because all of the radiation is not lost, but some is scattered toward other particles and rescattered in the direction of the receivers. In such cases, the measured attenuation will therefore be less than expected for a particular rainfall rate. If true this may account in part for the large scatter in some experiments (Medhurst, 1965).

Crane does not compute the magnitude of the enhanced signal. However, he does compute the pathlength through rain at which multiple scattering becomes "important." Table 4 gives these distances as a function of frequency for a rainfall rate of 25.4 mm h^{-1}. For other rainfall rates the distances shown decrease inversely with rate. Clearly, if Crane is correct, multiple scattering must be considered even at 3 cm wavelength in the heavier rains.

A possible hint of such effects may be found in the results of de Bettencourt (1974) who has synthesized the empirical behavior of the relationship $A = KR^{\alpha}$ from an extensive review of experiments. He shows that the experimental values of α are generally smaller than the theoretical ones, increasingly so the smaller the wavelength for wavelengths $\lesssim 1.5$ cm. Such behavior would be consistent with that expected as a result of multiple scatter.

On the other hand, Hogg (1975) raises doubts about the significance of multiple scattering effects in the microwave band. He argues that since the scatter from raindrops is essentially isotropic, radiation scattered in the near forward direction contributes very little to a narrow beam receiving antenna. He also suggests that the typical spacing of about 10 cm between adjacent drops of about 2 mm diameter in a rain as intense as 100 mm h^{-1} is so great as to make multiple scattering negligible.

Nevertheless, at this stage we lack an adequate assessment of the quantitative effects of multiple scatter on the net observed attenuation. It is therefore important that calculations of multiple scatter be conducted to determine their significance and whether the A-R relations described here need to be corrected. If they are important and no corrections are made, our results would be applicable only to coherent transmission systems or to modest rain rates and short paths.

TABLE 3. Percent error of estimated R from true R as a function of α. All values positive.

			α		
$R(x)$	1	1.05	1.10	1.15	1.20
Parabolic	0	0.6	1.2	1.8	2.4%
Isosceles triangle	0	0.9	1.9	2.8	3.7%

TABLE 4. Path lengths through a rain of 25.4 mm h^{-1} at which multiple scattering becomes significant (after Crane, 1971).

Frequency (GHz)	10	15	20	25	30	35
Wavelength (cm)	3.0	2.0	1.5	1.2	1.0	0.86
Path length (km)	41	10	3.5	2.3	1.4	0.9

7. Some prior experiments

Medhurst (1965, 1967), Crane (1971) and de Bettencourt (1974) discuss a variety of prior experiments. Medhurst was struck by the wide scatter in attenuation versus rain rate data, and more particularly, by the fact that some measurements show attenuation values which exceed the theoretical maximum predicted from the Mie theory, the latter computed by using monodisperse drop size spectra with maximum attenuation cross section. He therefore questions the validity of the Mie theory.

Crane (1971) argues, however, that the tendency toward agreement (between theory and experiment) in experiments with short paths and dense raingage networks and differing amounts of disagreement in others suggests that the discrepancies are not due to inapplicability of Mie theory, but rather to an inadequacy in the use of meteorological data. Among other things, Crane notes that small intense showers are likely to intercept the path but their cores may not pass over the gages, thus giving an unexpectedly large attenuation for the observed rainfall. This would account, in part, for measurements larger than theoretical, but not for a systematically larger attenuation coefficient as has been observed in some experiments (Medhurst, 1967; Semplak and Turrin, 1969).

In one storm reported by Semplak and Turrin (1969), they observed a rather systematic increase in the "apparent" attenuation coefficient at 18.5 GHz (1.62 cm) for rain rates up to 50 mm h^{-1}. They attributed this to an updraft of 1 m s^{-1} which would slow the raindrops and produce larger concentrations and effective rain rates in the elevated path than is indicated by the raingages at the surface. Their arguments are made plausible by the accompanying surface wind data which show very strong low-level convergence within the shower. Similarly, the systematically larger than theoretical attenuations observed by Anderson *et al.* (1947) at 1.25 cm in orographic rainfall in Hawaii (and one source of Medhurst's concern) could be attributed to upslope air motions.

Unauthenticated | Downloaded 04/21/25 09:47 PM UTC

However, another alternative which might well explain the systematic discrepancies in some experiments is the effect of differential attenuation with polarization which, as was shown in Section 7 for $\lambda = 0.86$ cm, increases nearly linearly with rainfall rate. Thus, in those cases where experimenters made measurements with horizontal polarization and compared the results to theoretical attenuation values for spherical drops, the actual attenuation would exceed theory in a systematic fashion. However, this cannot explain the results of Semplak and Turrin because they employed vertical polarization.

Among the most careful experiments conducted are those of Godard (1965) and Harrold (1967). Godard used a 0.86 cm radar viewing a corner reflector at 2.8 km and a single raingage at 2.0 km. However, he was careful to use only rainfalls which were horizontally homogeneous over the path as observed by the radar. For rates between 1.5 and 9.5 mm h^{-1} he found a mean attenuation coefficient of 0.23 dB km^{-1} (mm $h^{-1})^{-1}$ in excellent accord with our predicted value. At rates <1.5 mm h^{-1}, the attenuation coefficient increased with decreasing rate. His comprehensive error analysis forced him to the conclusion that this was due to systematically increasing underestimates of rainfall by the gage as the rate decreased.

Harrold (1967) measured the relative attenuation at 0.86 cm between two corner reflectors spaced 6.9 km apart, the nearest being 26.5 km from the radar. Eight raingages were deployed between the reflectors. Harrold found that about 40% of his 1008 1 min duration observations exceeded the theoretical maximum values, but the occurrence of both larger and smaller than theoretical values decreased with both the number and total duration of such observations. In the light of our previous discussion concerning the effects of updrafts and localized showers on overestimating the attenuation, it is not surprising to find the shorter duration observations producing apparently larger than expected attenuations, and occasionally smaller ones. Harrold found a mean attenuation coefficient of 0.26 dB km^{-1} (mm $h^{-1})^{-1}$, about 13% higher than our predicted value. This difference is readily attributed to his neglect of the effects of attenuation by oxygen and water vapor. Nevertheless, out of 23 cases lasting from 14 to 395 min, and covering 1 min path average rates up to 14 mm h^{-1}, only six produced path- and time-integrated total rain accumulations outside the range of $\pm 20\%$ of that indicated by the gages, and the average error for all cases was only 13.7%.

8. Summary and conclusions

We have shown that at a wavelength of about 0.9 cm, the attenuation A is linearly related to rainfall rate R and is essentially independent of the drop size distribution and temperature. This occurs because at this wavelength the weighting function for contributions of drops of diameter D to R has a form almost identical to that of $Q_t(D)$, the extinction coefficient, which is the weighting function for the drop contributions to A. At 0.86 cm, empirical results show average errors of less than 10% in estimates of R from A. As the wavelength increases to 3.2 cm, the exponent α in $A = KR^{\alpha}$ increases to 1.16 (at $T = 10°C$) and the errors of estimate of R increase to about 20%. This is still less than half the typical error in estimating R from radar reflectivity. However, at 3.2 cm corrections must be made for the temperature dependence of the A-R law.

Various practical methods of measuring path- and area-averaged R have been studied. Over a 30 km path, radar methods using standard targets at 0.86 and 1.25 cm are incapable of measuring $\bar{R}$ in excess of about 9 and 20 mm h^{-1}, respectively, because of excessive attenuation. The radar methods fail at $\bar{R} \gtrsim 40$ mm h^{-1} at 1.778 cm, but are useful for all realistic rates at 3.2 cm. One-way methods between transmitter and receiver are the most suitable in terms of maximum measurable $\bar{R}$. A wavelength between 1.5 and 2 cm appears to provide a reasonable compromise between maximum path $\bar{R}$ and minimum errors. The choice of wavelength depends upon the path and area to be covered, the maximum rates to be measured and the accuracy desired. The methods may be extended to paths between the ground and aircraft or satellites. To measure $\bar{R}$ properly, measurements must be made at both horizontal and vertical polarization due to the increasing differential attenuation resulting from the larger nonspherical raindrops.

Some prior experiments are reviewed. Good results have generally been obtained on short paths with adequate numbers of gages. Much wider scatter has been observed in other experiments and occasionally, attenuation has been found to exceed theoretical maximum values. The latter are explainable either in terms of the sparsity of gages which tend to underestimate the true path rainfall in showery conditions, or by updrafts which produce greater water densities aloft than in the gages. Apparent excess attenuation may also be measured when using horizontal polarization in comparison to the theory for spherical drops. The converse may occur when using vertical polarization. One important problem in need of resolution is the effect of multiple scatter on the received signal. Authors are in conflict concerning the importance of this effect.

REFERENCES

Anderson, L. J., J. P. Day, C. H. Freres and A. P. D. Stokes, 1947: Attenuation of 1.25 cm radiation through rain. *Proc. IRE*, 35, 351–354.

Atlas, D., 1964: Advances in radar meteorology. *Advances in Geophysics*, Vol. 10, Academic Press, 317–478.

Unauthenticated | Downloaded 04/21/25 09:47 PM UTC

——, and C. W. Ulbrich, 1974: The physical basis for attenuation-rainfall relationships and the measurement of rainfall parameters by combined attenuation and radar methods. *J. Rech. Atmos.*, **8**, 175–298.

——, R. C. Srivastava and R. S. Sekhon, 1973: Doppler radar characteristics of precipitation at vertical incidence. *Rev. Geophys. Space Phys.*, **11**, 1–35.

Chisholm, J. P., 1963: Frequency shift reflection system. U. S. Patent No. 3,108,275, issued 22 October 1963.

Collis, R. T. H., and M. G. H. Ligda, 1961: A radar raingauge. *Preprints 9th Radar Meteorology Conf.*, Kansas City, Amer. Meteor. Soc., 391–395.

Crane, R. K., 1971: Propagation phenomena affecting satellite communication systems operating in the centimeter and millimeter wavelength bands. *Proc. IEEE*, **59**, 173–188.

de Bettencourt, J. T., 1974: Statistics of millimeter-wave rainfall attenuation. *J. Rech. Atmos.*, **8**, 89–119.

Drufuca, G., 1974: Rain attenuation statistics for frequencies above 10 GHz from radar observations. *J. Rech. Atmos.*, **8**, 413–420.

Eccles, P. J., and E. A. Mueller, 1971: X-band attenuation and liquid water content estimation by a dual-wavelength radar. *J. Appl. Meteor.*, **10**, 1252–1259.

Godard, S., 1965: Propriétés de l'atténuation par la pluie des ondes radioeléctriques dans la bande 0.86 cm. *J. Rech. Atmos.*, **2**, 121–167.

Gunn, R., and G. D. Kinzer, 1949: The terminal velocity of fall for water droplets in stagnant air. *J. Meteor.*, **6**, 243–248.

Harrold, T. W., 1967: The attenuation of 8.6 mm wavelength radiation in rain. *Proc. Inst. Elec. Eng. London*, **114**, 201–203.

Hogg, D. C., 1975: The role of rain in satellite communications. *Proc. IEEE*, **63**, 1308–1331.

Joss, J., and A. Waldvogel, 1967: Ein Spektrograph für Niederschlagstropfen mit automatischer Auswertung. *Pure Appl. Geophys.*, **68**, 240–246.

——, and ——, 1970: A method to improve the accuracy of radar measured amounts of precipitation. *Preprints 14th Radar Meteorology Conf.*, Tucson, Amer. Meteor. Soc., 237–238.

Kelkar, V. N., 1961: Size distribution of raindrops (Part III). *Indian J. Meteor. Geophys.*, **12**, No. 4, 553–559.

Lenhard, R. W., 1974: Precipitation intensity and extent. *J. Rech. Atmos.*, **8**, 375–384.

Marshall, J. A., and W. M. K. Palmer, 1948: The distribution of raindrops with size. *J. Meteor.*, **5**, 165–166.

Medhurst, R. G., 1965: Rainfall attenuation of centimeter waves: Comparison of theory and measurement. *IEEE Trans. Antennas Propagat.*, **AP-13**, 550–564.

——, 1967: Discussion of prediction of rainfall attenuation near 11 GHz and attenuation-rainfall measurements at 8.6 mm. *Proc. Inst. Elec. Eng. London*, **114**, 1849–1850.

Oguchi, T., and Y. Hosoya, 1974: Differential attenuation and differential phase shift of radio waves due to rain: Calculations at microwave and millimeter wave regions. *J. Rech. Atmos.*, **8**, 121–127.

Ryde, J. W., 1947: The attenuation and radar echoes produced at centimeter wavelengths by various meteorological phenomena. *Meteorological Factors in Radio Wave Propagation*, Physical Society of London, 169–189.

Sekhon, R. S., and R. C. Srivastava, 1971: Doppler radar observations of drop-size distribution in a thunderstorm. *J. Atmos. Sci.*, **28**, 983–994.

Semplak, R. A., and R. H. Turrin, 1969: Some measurements of attenuation by rainfall at 18.5 GHz. *Bell System Tech. J.*, **48**, 1767–1787.

Spilhaus, A. F., 1948: Raindrop size, shape and falling speed. *J. Meteor.*, **5**, 108–110.

Ulbrich, C. W., and D. Atlas, 1977a: The rain parameter diagram: methods and applications. *J. Geophys. Res.* (in press).

——, and ——, 1977b: A method for measuring precipitation parameters using radar reflectivity and optical extinction. *Ann. Télécommun.* (in press).

Wexler, R., and D. Atlas, 1963: Radar reflectivity and attenuation of rain. *J. Appl. Meteor.*, **2**, 276–280.

Unauthenticated | Downloaded 04/21/25 09:47 PM UTC